Synthesis, Structure, and Properties of Aromatic Ring-Layered Polymers Containing Ferrocene as a Terminal Unit

AUTHOR(S):

Morisaki, Yasuhiro; Murakami, Takuya; Chujo, Yoshiki

Synthesis, Structure, and Properties of Aromatic Ring-Layered Polymers Containing Ferrocene as a Terminal Unit

Yasuhiro Morisaki,* Takuya Murakami, and Yoshiki Chujo*

Department of Polymer Chemistry, Graduate School of Engineering, Kyoto University

Katsura, Nishikyo-ku, Kyoto 615-8510, Japan

To whom correspondence should be addressed. E-mail: ymo@chujo.synchem.kyoto-u.ac.jp; chujo@chujo.synchem.kyoto-u.ac.jp

[2.2]Paracyclophane-layered polymers **4a** and **4b** end-capped by ferrocene and [2.2]paracyclophane, respectively, were synthesized by using a xanthene skeleton as a scaffold. Two model compounds, 4,5-bis(ferrocenylethynyl)-9,9-dimethylxanthene **7** and pseudo-*p*-bis(4-ferrocenylethynyl-9,9-dimethylxanthen-5-yl)[2.2]paracyclophane **8**, comprising ferrocenes arranged in a face-to-face manner were also prepared. According to the X-ray molecular structure of compound **8**, [2.2]paracyclophane between the ferrocenes had sufficient space for twisting and there was no interaction between two ferrocenes via [2.2]paracyclophane in the ground state. These polymers exhibited blue–light emission originating from the layered cyclophanes; however, the photoluminescence intensity of polymer **4a** was lower than that of polymer **4b**. The fluorescence emission of polymer **4a** was effectively quenched by the end-capping ferrocene group.

KEY WORDS: Aromatic ring-layered polymers; [2.2]paracyclophane; xanthene; energy transfer

1. INTRODUCTION

In organic materials, hole, electron, and energy transfers occur via a through-space as well as through-bond interaction of π-conjugated systems. These transfers occur via aromatic rings of π-conjugated molecules or polymers. A π-π stacking structure and orientation of aromatic rings play an important role in enabling effective charge or energy transfer. Although the syntheses of new conjugated polymers have been intensively pursued in recent years [1–3], few reports have described conjugated polymers consisting of layered aromatic rings via the through-space interaction of the π-π stacking [4–16]. Conjugated polymers and molecular wires such as poly(phenylene-ethynylene)s (PPEs) and oligothiophenes synthesized thus far consist of sp or sp^2 carbon frameworks [17–26].

Previously, we reported the synthesis and characterization of through-space conjugated polymers possessing [2.2]paracyclophane as a key repeating unit in the main chain [27–39]. We found that the [2.2]paracyclophane-containing polymers showed an extension of the conjugation length not only by the through-bond conjugation but also by the through-space conjugation of two-layered aromatic rings of [2.2]paracyclophane. During our investigation of the synthesis of through-space conjugated polymers, we developed a new methodology for the construction of benzene-ring-layered polymers comprising [2.2]paracyclophanes aligned face to face by employing xanthene skeleton as a scaffold [12,13]. While π-π stacking among the cyclophane units of the polymers was ineffective in the ground state because of the relatively long distance for the π-π interaction among neighboring cyclophane units, fluorescence resonance energy transfer (FRET) occurred from the layered cyclophane to the end–capping aromatic groups [13]. We thus decided to investigate the structural aspect of the polymers by using model compounds and elucidate the optical property of the polymers end-capped by ferrocenes in the excited state. Herein, we report the synthesis, structural characterization, and optical properties of the aromatic-ring-layered polymers containing ferrocene as a terminal unit.

2. RESULTS AND DISCUSSION

Scheme 1 illustrates the synthetic procedure of polymers **4a** and **4b** catalyzed by $Pd(PPh_3)_4$/CuI from monomers 4,16-diethynyl[2.2]paracyclophane **1** [40,41], 2,7-di-*tert*-butyl-4,5-diiodo-9,9-dimethylxanthene **2** [12,13], and ethynylferrocene **3a** or ethynyl[2.2]paracyclophane **3b** [40,41] as end-capping groups. The results of polymerizations are summarized in Table I. In both cases, the reactions proceeded smoothly to produce the corresponding polymers **4a** and **4b** in good yields. The number-average molecular weights (M_n) of polymers **4a** and **4b** were estimated by the ^{1}H NMR integral ratio between ferrocene and *tert*-butyl protons and that between bridged methylene and *tert*-butyl protons, respectively. In the case of Entry 1, M_n was estimated to be 8000 (n = 12.6), indicating that approximately 13 cyclophanes were incorporated into the polymer main chain; in other words, 26 benzene rings were aligned on the xanthene units.

(Scheme 1 and Table I)

Two related model compounds **7** and **8** were prepared according to the reactions shown in Schemes 2 and 3, respectively. The structures of compounds **7** and **8** were successfully confirmed by X-ray crystallographic studies, as shown in Figures 1 and 2. In the X-ray structure of **7** (Figure 1), the xanthene skeleton is curved in the top view. The cyclopentadienyl rings of ferrocenes and the xanthene moiety have a twisted conformation as expected, and the dihedral angles of the cyclopentadienyl rings and xanthene rings are approximately 86.4° and 60.9°, respectively, as shown in the top view. The twisted structure was ascribed to the steric hindrance of the cyclopentadienyl rings attached to the 4,5-position of a xanthene skeleton. Two cyclopentadienyl rings were arranged in a face-to-face manner [42–49]. While the distance between the 4-position and the 5-position of xanthene was 4.561 Å, the shortest distance between the intramolecular cyclopentadienyl rings was 3.491 Å, as shown in the side view. The distance (3.491 Å) is approximately equal to the sum of the van der Waals radius of an sp^2 carbon

(3.40 Å). In the crystal packing structure of **7**, the molecules were slipped, indicating that there is no intermolecular π-π stacking among the cyclopentadienyl rings.

(Scheme 2 and Figure 1)

The molecular structure of **8** possessing the [2.2]paracyclophane unit between two ferrocenes is depicted in Figure 2. The side view and top view of a part of the molecule are shown. The cyclopentadienyl rings of **8** are twisted in a similar manner to those of **7**, and the torsion angle of the cyclopentadienyl and xanthene rings is 88.8°. A remarkable feature of the structure is the conformation of the central [2.2]paracyclophane unit. One benzene ring of [2.2]paracyclophane and xanthene are almost on the same plane with a torsion angle of 166.0°. [2.2]Paracyclophane prefers π-conjugation with xanthene rings to avoid steric repulsion with two ferrocenes, which results in the deviation from linearity of the acetylene unit with C≡C–Ar bond angles of 159.0° and 173.6°, as shown in Figure 2. Complete rotation of the [2.2]paracyclophane unit in the polymer main chain is considered to be difficult because [2.2]paracyclophane containing two ethylene chains is layered in polymer **4a**; this is different in the case of compound **8** consisting of one [2.2]paracyclophane and two small cyclopentadienyl rings. The polymers undoubtedly have sufficient space so that [2.2]paracyclophane can twist, and thus, the UV spectra of polymers are independent of the number of layered [2.2]paracyclophanes [12,13].

(Scheme 3 and Figure 2)

In the ^{1}H NMR spectrum of **7**, slight downfield shifts of internal cyclopentadienyl protons were observed. The internal cyclopentadienyl proton signals of **7** appeared at 4.09 and 4.41 ppm (at 4.19 ppm for the external cyclopentadienyl protons), as shown in Figure S5 in Supporting Information, whereas those of **6** appeared at 4.25 and 4.61 ppm (at 4.27 ppm for the external cyclopentadienyl protons). It is considered that the ring current effect between the internal

cyclopentadienyl rings in solution is small and that two ferrocenes in compound **7** move freely without forming of a π-stacked structure in solution. In order to examine the redox behavior of **7** in solution, cyclic voltammetry was carried out (Figure 3). Compound **7** exhibited a reversible oxidation wave at approximately E_{pa} = 0.13 V as a shoulder peak, E_{pa} = 0.22 V, and $E_{1/2}$ = 0.12 V (*vs* Fc/Fc^{+}) arising from the stepwise oxidation of two ferrocenes via the mixed valence state. We have considered that this result was due to the through-bond interaction rather than the through-space interaction, *i.e.*, polar/π interaction [50–54]. Incidentally, compound **8** and polymer **4a** exhibited only a reversible oxidation peak at $E_{1/2}$ = 0.077 V and 0.070 V (*vs* Fc/Fc^{+}) [12,13], respectively (Figures 4 and 5); thus, there was no evidence of interactions between terminal ferrocenes via the thorough-space interaction in the ground state.

In order to investigate the properties of aromatic-ring-layered polymers in the excited state, photoluminescence studies were carried out. Figure 6 shows not only the absorption spectra of polymers **4a** and **4b** in dilute $CHCl_3$ solutions (1.0×10^{-5} M/layered-cyclophane unit) but also their photoluminescence spectra in dilute $CHCl_3$ solutions (5.0×10^{-7} M/layered-cyclophane unit). Since polymers **4a** and **4b** have almost the same number of [2.2]paracyclophane units, they exhibit similar absorbance at around 290 and 335 nm (Figure 6, left).

(Figure 6)

The polymers were excited at 335 nm in dilute $CHCl_3$ solution, and they exhibited almost identical photoluminescence spectra with peak maxima at around 410 nm (Figure 6, right), which were derived from the emission of the layered [2.2]paracyclophane units. However the peak intensity of polymer **4a** was lower than that of polymer **4b**, in spite of the same absorbance values. We confirmed that this concentration was diluted sufficiently to avoid intermolecular interactions according to the concentration effect of the photoluminescence spectra (Figure S13 in Supporting Information). Therefore, the terminal ferrocene units in the polymer **4a** backbone quenched the photoluminescence via the through-space interaction. The solvent polarity

dependence of the photoluminescence was examined for polymers **4a** and **4b**, and no solvent effects were observed in dilute cyclohexane, $CHCl_3$, THF, CH_2Cl_2, and DMF (Figure S14 in Supporting Information). This result implies that energy transfer from the layered cyclophanes to terminal ferrocenes occurred exclusively rather than electron transfer in the present system. The energy transfer efficiency was roughly estimated to be 38% from the photoluminescence quantum efficiencies of the polymers.

(Figure 7)

(Figure 8)

Figure 7 shows the fluorescence emission spectra of [2.2]paracyclophane-terminated polymer **4b** with additional ferrocene acting as an emission-quencher in $CHCl_3$. To the solution of **4b**, 10 or 100 eq. of ferrocene with respect to the [2.2]paracyclophane unit in the polymer main chain was added. By the addition of 10 eq. of ferrocene, only 3% of the emission of polymer **4b** was quenched. Additionally, 25% of the emission of **4b** was quenched in spite of the addition of 100 eq. of ferrocene, whereas 38% of the emission of **4a** was quenched by only two ferrocenes at the polymer chain ends (*ca.* 0.16 eq. of ferrocene on the basis of M_n = 8000). Stern-Volmer coefficient (K_{sv}) of polymer **4a** was approximately 1.4×10^3 times larger than the addition of ferrocenes to polymer **4b**, as shown in Figure 8. Thus, a significant polymer effect, *i.e.*, concentration effect [55–61], was achieved by the incorporation of the ferrocenes into the polymer, leading to effective energy transfer from the layered cyclophanes to the ferrocenes.

3. CONCLUSIONS

[2.2]Paracyclophane-layered polymers end-capped by ferrocene and [2.2]paracyclophane were synthesized by employing the xanthene skeleton as a scaffold. In order to investigate the structural aspect of the aromatic-ring-layered polymers, two model compounds comprising face-to-face ferrocenes were prepared. The layered [2.2]paracyclophane in the polymer main

chain had sufficient space for twisting, which leads to ineffective π-π stacking among the cyclophane units of the polymers in the ground state. The polymer end-capped by the ferrocene group exhibited the blue-light emission derived from the layered cyclophanes; however, the photoluminescence intensity of polymer **4a** was lower than polymer **4b** end-capped by the [2.2]paracyclophane group. The fluorescence emission of the polymer end-capped by ferrocene was effectively quenched due to the through-space energy transfer from the main chain to the end-capping ferrocene group. Thus, in the excited state, the [2.2]paracyclophane-layered polymer can act as a molecular wire for the transmission of energy and electrons. Further studies on the introduction of various aromatic compounds as the end-capping group in the [2.2]paracyclophane-layered polymers are currently under way; these studies will lead to the development of a molecular wire consisting of layered aromatic rings.

4. EXPERIMENTAL SECTION

4.1. General

^{1}H and ^{13}C NMR spectra were recorded on a JEOL JNM-EX400 instrument at 400 and 100 MHz, respectively. The chemical shift values were expressed relative to Me_4Si as an internal standard. High-resolution mass spectra (HRMS) were obtained on a JEOL JMS-SX102A spectrometer. Analytical thin-layer chromatography (TLC) was performed with silica gel 60 Merck F_{254} plates. Column chromatography was performed with Merck aluminium dioxide 90 Basic and Wakogel C-300 silica gel. Recyclable preparative high-performance liquid chromatography (HPLC) was carried out on a Japan Analytical Industry LC-918R (JAIGEL 1H and 2H columns) or LC-9204 (JAIGEL 2.5H and 3H columns) instrument using $CHCl_3$ as an eluent. Gel permeation chromatography (GPC) was carried out on a TOSOH 8020 (TSKgel G3000HXL column) instrument using $CHCl_3$ as an eluent after calibration with standard polystyrene samples. UV-vis absorption spectra were obtained on a SHIMADZU UV3600 spectrophotometer. Photoluminescence spectra were obtained on a Perkin-Elmer LS50B luminescence spectrometer. Cyclic voltammetry (CV) was carried out on a BAS CV-50W electrochemical analyzer in CH_2Cl_2 containing 0.1 M Bu_4NPF_6 with a glassy carbon working electrode, a Pt counter electrode, an Ag/Ag^+ pseudo-reference electrode at a scan rate of 100 mV/s. Elemental analysis was performed at the Microanalytical Center of Kyoto University.

4.2. Materials

THF, Et_2O, and Et_3N were purchased and purified by passage through purification column under Ar pressure [62]. $Pd(PPh_3)_4$, CuI, and ethynylferrocene **3a** were obtained commercially, and used without further purification. Pseudo-*p*-diethynyl[2.2]paracyclophane **1** was prepared from commercially available [2.2]paracyclophane as described in the literature [34]. 4-Ethynyl[2.2]paracyclophane **3b** [40] and 4,5-diiodo-9,9-dimethylxanthene **5** [63] were prepared as described in the literature. All reactions were performed under Ar atmosphere.

4.3. X-ray crystal structure analysis

Intensity data were collected on a Rigaku R-AXIS RAPID imaging plate area detector with graphite monochromated Mo Ka radiation (λ = 0.71069 Å) at –180°C. The structures were solved by direct method (SIR97) [64] and refined by full-matrix least-squares procedures based on F^2 (SHELX-97) [65].

4.4. Synthesis and Characterization

4.4.1 Polymerization

A typical procedure is as follows. Pseudo-*p*-diethynyl[2.2]paracyclophane **1** (23.1 mg, 0.090 mmol), 2,7-di-*tert*-butyl-4,5-diiodo-9,9-dimethylxanthene **2** (57.4 mg, 0.100 mmol), 4-ethynyl[2.2]paracyclophane **3b** (4.6 mg, 0.020 mmol), $Pd(PPh_3)_4$ (11.6 mg, 0.010 mmol) and CuI (1.9 mg, 0.010 mmol) were placed in a 10 mL Pyrex tube equipped with a magnetic stirrer and a reflux condenser. The equipment was purged with Ar, followed by adding THF (4.0 mL) and Et_3N (2.0 mL). The reaction was carried out at 50°C for 48 h. After cooling, the reaction mixture was diluted with $CHCl_3$, and washed with NH_3 aqueous solution, water, and brine. The organic layer was dried over Na_2SO_4. The organic layer was concentrated and reprecipitated from a large amount of methanol. The obtained polymer containing low molecular weight residues was purified by HPLC. The polymer was dried in vacuo to afford polymer **4b** as a yellow solid (47.1 mg, 79%).

Polymer 4a: Yield: 85%. ^{1}H NMR (CD_2Cl_2, 400 MHz): δ 1.35 (br, -*Bu*^{t}), 1.67 (br, -*Me*), 2.3–3.2 (br, *bridge methylene protons of cyclophane units*), 3.3–3.7 (br, *bridge methylene protons of cyclophane units*), 4.0–4.3 (br m, *protons of ferrocene units*), 6.0–7.1 (br, *aromatic protons of cyclophane units*), 7.3–7.7 (br m, *aromatic protons of xanthene units*).

Polymer 4b: Yield: 79%. ^{1}H NMR (CD_2Cl_2, 400 MHz): δ 1.1–1.4 (br, -*Bu*^{t}), 1.5–1.7 (br, -*Me*), 2.3–3.8 (br m, *bridge methylene protons of cyclophane units*), 6.0–7.0 (br, *aromatic protons of the cyclophane unit*s), 7.1–7.8 (br m, *aromatic protons of xanthene units*).

4.4.2 Synthesis of 2,7-Di-tert-butyl-4,5-diiodo-9,9-dimethylxanthene ***2***

To cooled solution (–5°C) of 4,5-dibromo-2,7-di-*tert*-butyl-9,9-dimethylxanthene (2.4 g, 5.0 mmol) in Et_2O (200 mL) was added *n*-BuLi (4.5 mL of 2.6 M hexane solution, 12 mmol)/TMEDA (2.0 mL) prepared in a dropping funnel dropwise under Ar. After 20 min, a solution of iodine (2.8 g, 11 mmol) in Et_2O (30 mL) was added dropwise over a period of 1 h at –20°C. This solution was stirred for 30 min at 0°C and for 2 h at room temperature. The reaction was quenched by the addition of saturated aqueous Na_2SO_3 (150 mL). The organic layer was separated and the aqueous layer was extracted with Et_2O several times. The combined organic layers were dried over $MgSO_4$. The solvent was removed on an evaporator to give the pale yellow solid residue, which was recrystallized from hot hexane to obtained pure **2** (2.0 g, 3.6 mmol, 70%) as a white crystal.

^{1}H NMR ($CDCl_3$, 400 MHz): δ 1.32 (s, -*Bu*^{t}, 18H), 1.62 (s, -*Me*, 6H), 7.33 (s, J = 2.2 Hz, *aromatic protons*, 2H), 7.47 (d, J = 2.2 Hz, *aromatic protons*, 2H); ^{13}C NMR ($CDCl_3$, 100 MHz): δ 31.4, 32.0, 34.5, 35.7, 77.2, 110.4, 121.5, 128.5, 131.1, 147.2. Anal. calcd for $C_{23}H_{28}I_2O$: C 48.10, H 4.91. Found: C 48.07, H 4.95.

4.4.3 Synthesis of 4-Ferrocenylethynyl-5-iodo-9,9-dimethylxanthene ***6*** *and 4,5-Bis(ferrocenylethynyl)-9,9-dimethylxanthene* ***7***

4,5-Diiodo-9,9-dimethylxanthene **5** (464 mg, 1.00 mmol), ferrocenylacetylene (210 mg, 1.00 mmol), $Pd(PPh_3)_4$ (58 mg, 0.05 mmol), and CuI (10 mg, 0.05 mmol) were placed in a 100 mL Pyrex flask equipped with a magnetic stirrer and a reflux condenser. The equipment was purged with Ar, followed by adding THF (20 mL) and Et_3N (20 mL). The reaction was carried out at 50°C for 24 h. After cooling, the reaction mixture was diluted with $CHCl_3$, and washed with NH_3 aqueous solution, water, and brine. The organic layer was dried over Na_2SO_4 and then concentrated to afford the crude product. This contained reactant and two products, which was purified by silica gel column chromatography (hexane/$CHCl_3$, v/v = 4/1 as an eluent) to afford **6** as a red solid (180 mg, 0.33 mmol, 33%) and **7** as a red crystal (163 mg, 0.26 mmol, 26%).

4-Ferrocenylethynyl-5-iodo-9,9-dimethylxanthene **6**: Yield: 33%. R_f = 0.42 (hexane/$CHCl_3$, v/v = 2/1). ^{1}H NMR (CDCl3, 400 MHz): δ 1.60 (s, *-Me*, 6H), 4.25 (t, *J* = 1.8 Hz, *ferrocene protons*, 2H), 4.27 (s, *ferrocene protons*, 5H), 4.61 (t, *J* = 1.8 Hz, *ferrocene protons*, 3H), 6.84 (t, *J* = 7.8 Hz, *xanthene proton*, 1H), 7.05 (t, *J* = 7.8 Hz, *xanthene proton*, 1H), 7.33 (dd, *J* = 7.8, 1.5 Hz, *xanthene proton*, 1H), 7.37 (dd, *J* = 7.8, 1.5 Hz, *xanthene proton*, 1H), 7.41 (dd, *J* = 7.8, 1.5 Hz, *xanthene proton*, 1H), 7.72 (dd, *J* = 7.8, 1.5 Hz, *xanthene proton*, 1H). ^{13}C NMR ($CDCl_3$, 100 MHz): δ 32.0, 34.7, 65.7, 68.8, 70.0, 71.7, 81.6, 85.0, 93.6, 112.8, 123.2, 124.9, 125.2, 126.1, 130.3, 130.9, 131.2, 137.5, 149.5, 150.8. HRMS (FAB): m/z calcd for $C_{27}H_{21}OFeI$ (M^+): 543.9987. Found: 543.9984. Anal. calcd for $C_{27}H_{21}OFeI$: C 59.59; H 3.89. Found: C 59.32; H 3.87.

4,5-Bis(ferrocenylethynyl)-9,9-dimethylxanthene **7**: Yield: 26%. R_f = 0.17 (hexane/$CHCl_3$, v/v = 2/1). ^{1}H NMR ($CDCl_3$, 400 MHz) : δ 1.62 (s, *-Me*, 6H), 4.08 (t, *J* = 1.7 Hz, *ferrocene protons*, 4H), 4.19 (s, *ferrocene protons*, 10H), 4.41 (t, *J* = 1.6 Hz, , *ferrocene protons*, 4H), 7.05 (t, *J* = 7.7 Hz, *xanthene protons*, 2H), 7.35 (dd, *J* = 7.7, 1.2 Hz, *xanthene protons*, 2H), 7.43 (dd, *J* = 7.7, 1.2 Hz, *xanthene protons*, 2H). ^{13}C NMR ($CDCl_3$, 100 MHz): δ 32.4, 34.1, 65.6, 68.6, 69.9, 71.9, 81.3, 92.8, 112.6, 122.8, 125.6, 130.1, 132.0, 150.2. HRMS (FAB): m/z calcd for $C_{39}H_{30}OFe_2$ (M^+): 626.0995. Found: 626.0992. Anal. calcd for $C_{39}H_{30}OFe_2$: C 74.79; H 4.83. Found: C 75.07; H 4.87.

*4.4.4 Synthesis of Pseudo-p-bis(4-ferrocenylethynyl-9,9-dimethylxanthen-5-yl) [2.2]paracyclophane **8***

4-Ferrocenylethynyl-5-iodo-9,9-dimethylxanthene **6** (103 mg, 0.190 mmol), pseudo-*p*-diethynyl[2.2]paracyclophane **1** (24 mg, 0.095 mmol), $Pd(PPh_3)_4$ (11 mg, 0.010 mmol), CuI (2 mg, 0.010 mmol) were placed in a 30 mL Pyrex flask equipped with a magnetic stirrer and a reflux condenser. The equipment was purged with Ar, followed by adding THF (8.0 mL) and Et_3N (4.0 mL). The reaction was carried out at 50°C for 24 h. After cooling, the reaction mixture was diluted with $CHCl_3$, and washed with 10% NH_3 aqueous solution, water, and brine.

The organic layer was dried over Na_2SO_4, and then concentrated in vacuo. The crude product was purified by silica gel column chromatography (hexane:$CHCl_3$, v/v = 2:1 as an eluent) and recrystallization from CH_2Cl_2 and hexane to afford **6** as an orange crystal (87 mg, 0.078 mmol, 82%).

^{1}H NMR ($CDCl_3$, 400 MHz): δ 1.67 (s, *-Me*, 12H), 2.74-2.67 (m, 2H, *bridge methylene protons of the cyclophane unit*), 2.87-2.80 (m, 2H, *bridge methylene protons of the cyclophane unit*), 3.15-3.08 (m, 2H, *bridge methylene protons of the cyclophane unit*), 3.74-3.68 (m, 2H, *bridge methylene protons of the cyclophane unit*), 3.92-3.90 (m, *ferrocene protons*, 2H), 3.94-3.92 (m, *ferrocene protons*, 2H) , 4.07 (s, *ferrocene protons*, 10H) , 4.21-4.19 (m, *ferrocene protons*, 2H) , 4.25-4.24 (m, *ferrocene protons*, 2H) , 6.39 (d, J = 7.8 Hz, *cyclophane protons*, 2H) , 6.50 (d, J = 1.7 Hz, *cyclophane protons*, 2H) , 7.00 (2H, dd, J = 7.8, 1.7 Hz, *cyclophane protons*, 2H), 7.05 (t, J = 7.7 Hz, *xanthene protons*, 2H), 7.14 (t, J = 7.7 Hz, *xanthene protons*, 2H), 7.37 (dd, J = 7.7, 1.6 Hz, *xanthene protons*, 2H) , 7.42 (dt, J = 7.7, 1.6 Hz, *xanthene protons*, 4H), 7.58 (dd, J = 7.7, 1.6 Hz, *xanthene protons*, 2H). ^{13}C NMR ($CDCl_3$, 100 MHz): δ 32.4, 32.5, 33.8, 34.2, 34.3, 65.3, 68.6, 69.8, 71.8, 81.2, 88.7, 93.2, 94.6, 112.7, 112.8, 122.9, 123.0, 124.7, 125.5, 126.0, 130.1, 130.2, 130.4, 131.9, 132.0, 133.2, 137.7, 139.3, 142.5, 150.0, 150.1. Anal. calcd for $C_{74}H_{56}O_2Fe_2$: C 81.62; H 5.18. Found: C 81.22; H 5.20.

^{1}H and ^{13}C NMR spectra of **2**, **4a–b**, **6**, **7**, and **8** summarized above as well as photoluminescence spectra of **4a–b** and X-ray crystallographic data of **7** and **8** are shown in Supporting Information. CCDC reference numbers of **7** and **8** are 702164 and 702165, respectively.

ACKNOWLEDGMENT

This work was supported by Grant-in-Aid for Creative Scientific Research of "Invention of Conjugated Electronic Structures and Novel Functions", No. 16GS0209, from the Ministry of Education, Culture, Sports, Science, and Technology, Japan.

REFERENCES AND NOTES

1. W. R. Salaneck, D. T. Clark, E. J. Samuelsen (eds), Science and Applications of Conducting Polymers, Adam Hilger, Bristol, (1991).

2. H. S. Nalwa, (ed), Handbook of Organic Conductive Molecules, Wiley, Chichester, (1997).

3. T. A. Skothim, R. L. Elsenbaumer, J. R. Reynolds (eds), Handbook of Conducting Polymers, 3rd ed. Marcel Dekker, New York, (2006).

4. T. Nakano, K. Takewaki, T. Yade, Y. Okamoto, J. Am. Chem. Soc. 123, 9182–9183 (2001).

5. T. Nakano, T. Yade, J. Am. Chem. Soc. 125, 15474–15484 (2003).

6. T. Nakano, T. Yade, M. Yokoyama, N. Nagayama, Chem. Lett. 33, 296–297 (2004).

7. T. Nakano, T. Yade, Y. Fukuda, T. Yamaguchi, S. Okumura, Macromolecules 38, 8140–8148 (2005).

8. T. Yade, T. Nakano, J. Polym. Sci. Part A: Polym. Chem. 44, 561–572 (2006).

9. T. Nakano, T. Yade, Chem. Lett. 37, 258–259 (2008).

10. A. García Martínez, J. Osío Barcina, A. de Fresno Cerezo, A.-D. Schlüter, J. Frahn, Adv. Mater. 11, 27–31 (1999).

11. S. A. Jenekhe, M. M. Alam, Y. Zhu, S. Jiang, a. V. Shevade, Adv. Mater. *19*, 536–542 (2007).

12. Y. Morisaki, Y. Chujo, Tetrahedron Lett. 46, 2533–2537 (2005).

13. Y. Morisaki, T. Murakami, Y. Chujo, Macromolecules 41, 5960–5963 (2008).

14. T. Otsubo, S. Mizogami, Y. Sakata, S. Misumi, Tetrahedron Lett. 13, 2927–2930 (1972).

15. T. Otsubo, S. Mizogami, I. Otsubo, Z. Tozuka, A. Sakagami, Y. Sakata, S. Misumi, Bull. Chem. Soc. Jpn. 46, 3519–3530 (1973).

16. M. Shibahara, M. Watanabe, T. Iwanaga, K. Ideta, T. Shinmyozu, J. Org. Chem. 72, 2865–2877 (2007).

17. K. Müllen (ed), Electronic Materials: The Oligomeric Approach, Wiley–VHC, Weinheim (1998).

18. J. M. Tour, Chem. Rev. 96, 537–554 (1996).

19. R. E. Martin, F. Diederich, Angew. Chem. Int. Ed. 38, 1350–1377 (1999).

20. J. M. Tour, Acc. Chem. Rec. 33, 791–804 (2000).

21. R. L. Carroll, C. B. Gorman, Angew. Chem. Int. Ed. 41, 4378–4400 (2002).

22. U. H. F. Bunz, Chem. Rev. 100, 1605–1644 (2000).

23. C. Weder, Poly(arylene ethynylene)s, Adv. Polym. Sci. Vol. 177 (2005).

24. D. Fichou (ed), Handbook of Oligo- and Polythiophenes, Wiley–VHC, Weinheim (1999).

25. T. Otsubo, Y. Aso, K. Takimiya, Bull. Chem. Soc. Jpn. 74, 1789–1801 (2001).

26. T. Otsubo, Y. Aso, K. Takimiya, J. Mater. Chem. 12, 2565–2575 (2002).

27. Y. Morisaki, Y. Chujo, Angew. Chem. Int. Ed. 45, 6430–6437 (2006).

28. Y. Morisaki, Y. Chujo, Prog. Polym. Sci. 33, 346–364 (2008).

29. Y. Morisaki, Y. Chujo, Macromolecules 35, 587–589 (2002).

30. Y. Morisaki, Y. Chujo, Chem. Lett. 194–195 (2002).

31. Y. Morisaki, T. Ishida, Y. Chujo, Macromolecules 35, 7872–7877 (2002).

32. Y. Morisaki, Y. Chujo, Polym. Bull. 49, 209–215 (2002).

33. Y. Morisaki, F. Fujimura, Y. Chujo, Organometallics 22, 3553–3557 (2003).

34. Y. Morisaki, Y. Chujo, Macromolecules 36, 9319–9324 (2003).

35. Y. Morisaki, Y. Chujo, Macromolecules 37, 4099–4103 (2004).

36. Y. Morisaki, T. Ishida, H. Tanaka, Y. Chujo, J. Polym. Sci. Part A: Polym. Chem. 42, 5891–5899 (2004).

37. Y. Morisaki, Y. Chujo, Bull. Chem. Soc. Jpn. 78, 288–293 (2005).

38. Y. Morisaki, N. Wada, Y. Chujo, Polym. Bull. 53, 73–80 (2005).

39. Y. Morisaki, N. Wada, Y. Chujo, Polymer 46, 5884–5889 (2005).

40. L. Bondarenko, I. Dix, H. Hinrichs, H. Hopf, Synthesis 16, 2751-2759 (2004).

41. H. Hopf, I. Dix, Synlett 1416–1418 (2006).

42. M. T. Lee, B. M. Foxman, M. Rosenblum, Organometallics 4, 539–547 (1985).

43. R. Arnold, B. M. Foxman, M. Rosenblum, W. B. Euler, Organometallics 7, 1253–1259 (1998).

44. R. Arnold, S. A. Matchett, M. Rosenblum, Organometallics 7, 2261–2267 (1988).

45. R. H. Herber, I. Nowik, M. Rosenblum, Organometallics 21, 846–851 (2002).

46. M. Iyoda, T. Okabe, M. Katada, Y. Kuwatani, J. Organomet. Chem. 569, 225–233 (1998).

47. H. M. Nugent, M. Rosenblum, P. Klemarczky, J. Am. Chem. Soc. 115, 3848–3849 (1993).

48. M. Rosenblum, H. M. Nugent, K.-S. Jang, M. M. Labes, W. Cahalane, P. Klemarczyk, W. M. Reiff, Macromolecules 28, 6330–6342 (1995).

49. R. D. A. Hudson, B. M. Foxman, M. Rosenblum, Organometallics 18, 4098–4106 (1999).

50. F. Cozzi, M. Cinquini, R. Annunziata, T. Dwyer, J. S. Siegel, J. Am. Chem. Soc. 114, 5729–5733 (1992).

51. F. Cozzi, M. Cinquini, R. Annunziata, J. S. Siegel, J. Am. Chem. Soc. 115, 5330–5331 (1993).

52. F. Cozzi, F. Ponzini, R. Annunziata, M. Cinquini, J. S. Siegel, Angew. Chem. Int. Ed. 34, 1019–1020 (1995).

53. R. Tsuji, K. Komatsu, K. Takeuchi, M. Shiro, S. Cohen, M. Rabinovitz, J. Phy. Org. Chem. 6, 435–444 (1993).

54. N. Kaneta, F. Mitamura, M. Uemura, Y. Murata, K. Komatsu, Tetrahedron Lett. 37, 5385–5388 (1996).

55. Q. Zhou, T. M. Swager, J. Am. Chem. Soc. 117, 7017–7018 (1995).

56. M. J. Marsella, P. J. Carroll, T. M. Swager, J. Am. Chem. Soc. 117, 9832–9841 (1995).

57. Q. Zhou, T. M. Swager, J. Am. Chem. Soc. 117, 12593–12602 (1995).

58. R. Deans, J. Kim, M. R. Machacek, T. M. Swager, J. Am. Chem. Soc. 122, 8565–8566 (2000).

59. A. Rose, C. G. Lugmair, T. M. Swager, J. Am. Chem. Soc. 123, 11298–11299 (2001).

60. J. Zheng, T. M. Swager, Adv. Polym. Sci. 177, 151–179 (2005).

61. S. W. Thomas, G. D. Joly, T. M. Swager, Chem. Rev. 107, 1339–1386 (2007).

62. A. B. Pangborn, M. A. Giardello, R. H. Grubbs, R. K. Rosen, R. F. J. Timmers, Organometallics 15, 1518–1520 (1996).

63. K. McWilliams, J. W. Kelly, J. Org. Chem. 61, 7408–7414 (1996).

64. A. Altomare, M. C. Burla, M. Camalli, G. Cascarano, C. Giacovazzo, A. Guagliardi, A. G. Moliteni, G. Polidori, Spagna, R. SIR97, A Program for the Automatic Solution and Refinement of Crystal Structures.

65. G. M. Sheldrick, SHELX97, Programs for Crystal Structure Analysis; University of Göttingen: Göttingen, Germany (1997).

Table I. Results of Polymerization

Entry	Polymer	Ar	Yield[a] /%	M_n	
				calcd.	found[b]
1	**4a**	ferrocenyl	85	5912	7980
2	**4b**	[2.2]paracyclophanyl	79	5956	4100

[a] Isolated yield after reprecipitation. [b] Estimated by the ^{1}H NMR integral ratio.

Figure Captions

Fig. 1. (A) ORTEP drawing of **7**. Top and side views are shown. Thermal ellipsoids are drawn at the 50% probability level. Hydrogen atoms are omitted for clarity. (B) Side view of crystal packing structure of **7**.

Fig. 2. (A) ORTEP drawing of **8** including the top view of a part of the molecule. Thermal ellipsoids are drawn at the 50% probability level. Hydrogen atoms and solvent (CH_2Cl_2) are omitted for clarity.

Fig. 3. Cyclic voltammogram of **7** in CH_2Cl_2 containing 0.1 M Bu_4NPF_6 as an electrolyte using a glassy carbon working electrode, a platinum wire counter electrode, and a Ag/Ag^+ reference electrode at a scan rate of 100 mV/s.

Fig. 4. Cyclic voltammogram of **8** in CH_2Cl_2 containing 0.1 M Bu_4NPF_6 as an electrolyte using a glassy carbon working electrode, a platinum wire counter electrode, and a Ag/Ag^+ reference electrode at a scan rate of 100 mV/s.

Fig. 5. Cyclic voltammogram of **4a** in CH_2Cl_2 containing 0.1 M Bu_4NPF_6 as an electrolyte using a glassy carbon working electrode, a platinum wire counter electrode, and a Ag/Ag^+ reference electrode at a scan rate of 100 mV/s.

Fig. 6. UV-vis absorption spectra of polymers **4a** and **4b** in $CHCl_3$ (1.0×10^{-5} M), and photoluminescence spectra of polymers **4a** and **4b** in $CHCl_3$ (5.0×10^{-7} M).

Fig. 7 Photoluminescence spectra of polymer **4b** (1.0×10^{-5} M) with ferrocene added in $CHCl_3$.

Fig. 8. Stern-Volmer plots of polymer **4a** (1.0×10^{-5} M) and polymer **4b** (1.0×10^{-5} M) with the fluorescence-quenching reagent (ferrocene) in $CHCl_3$. Q is a equivalent of the end-capping ferrocenes for polymer **4a** the and fluorescence quencher (ferrocene) for polymer **4b** based on the [2.2]paracyclophane unit.

Scheme 1

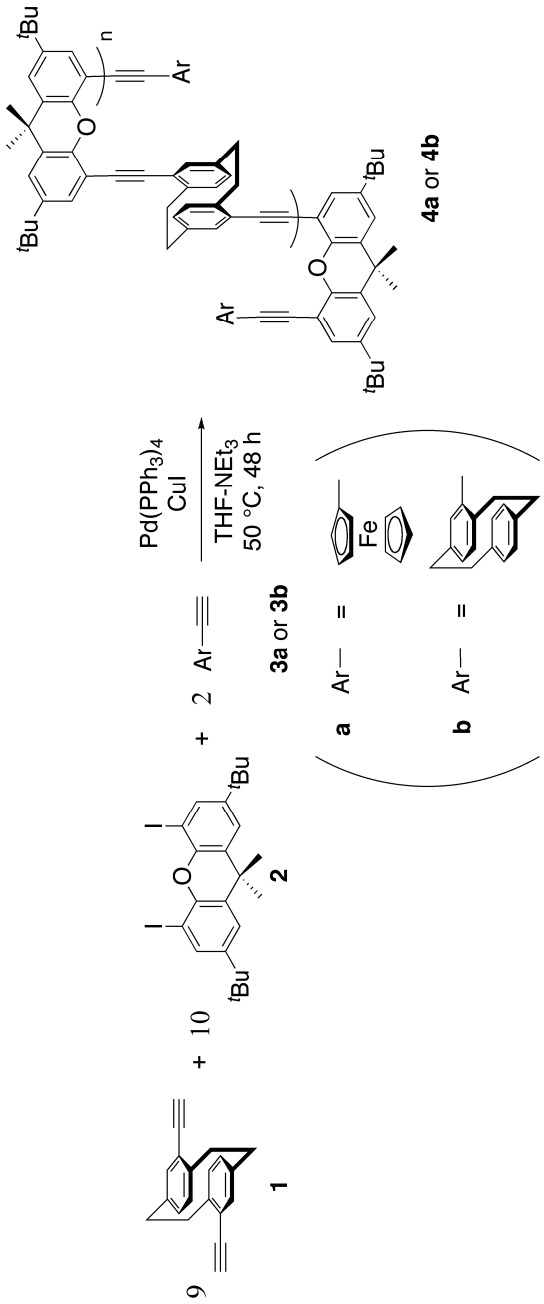

Scheme 2

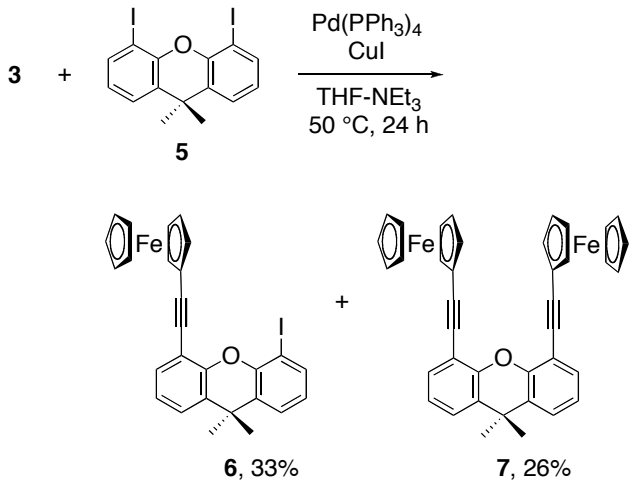

Scheme 3

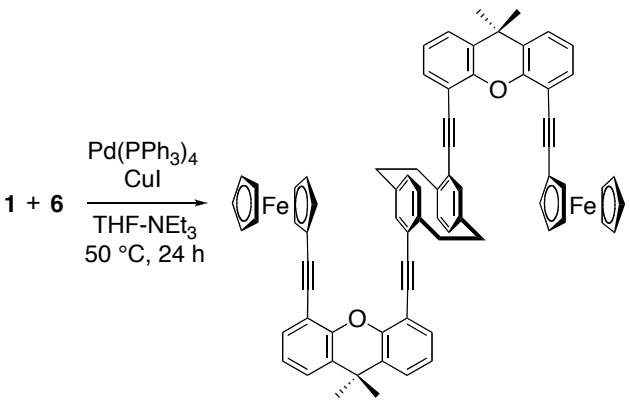

8, 82%

Figure 1

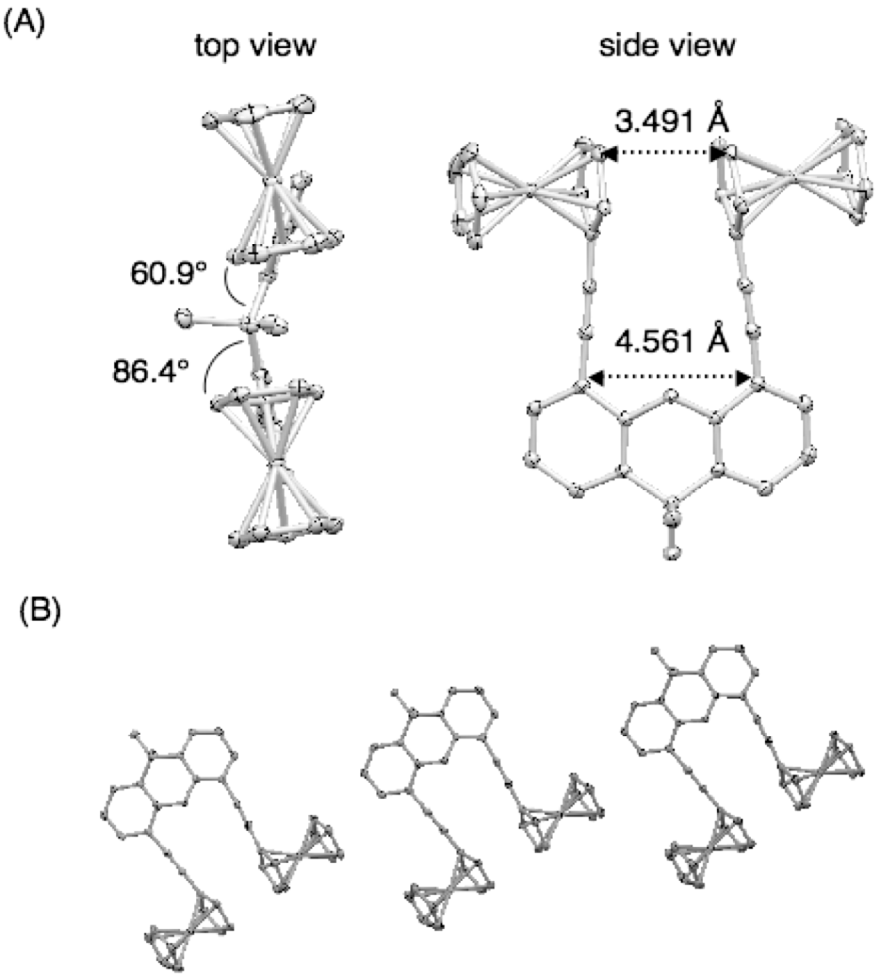

Figure 2

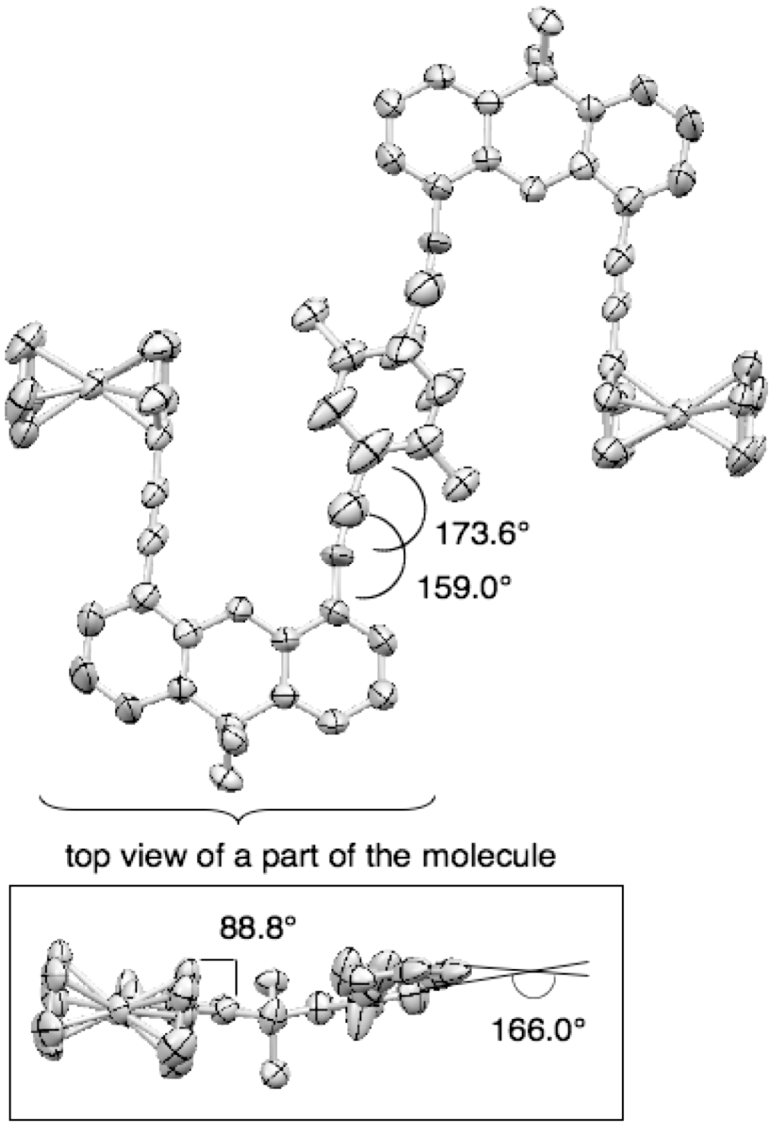

Figure 3

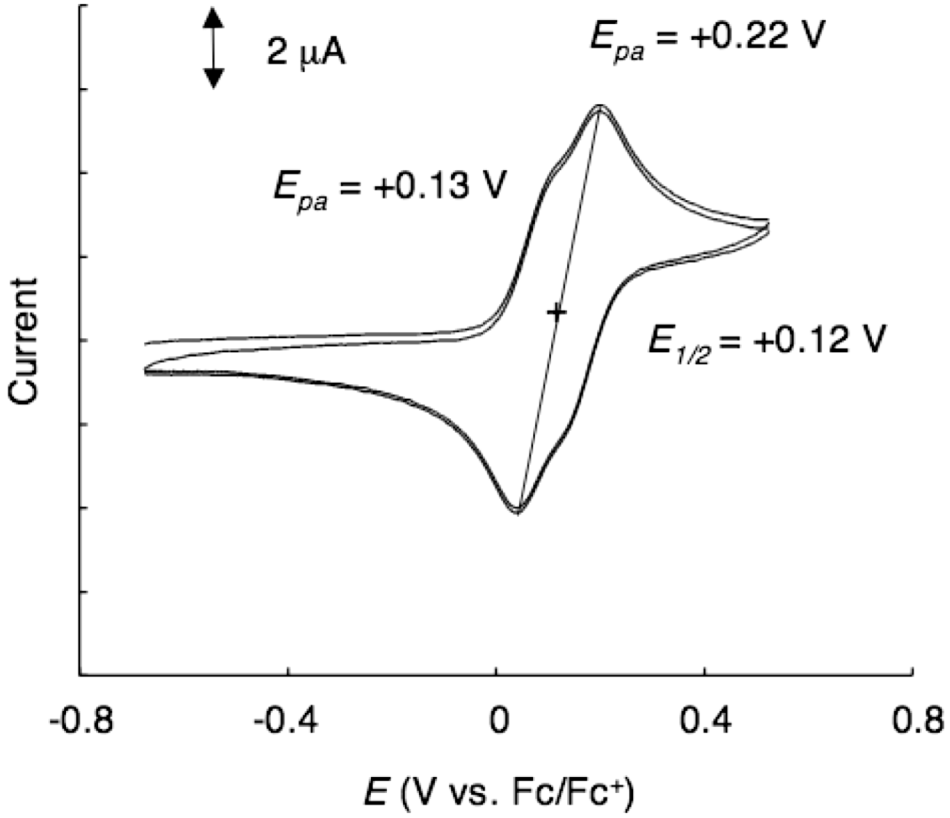

Figure 4

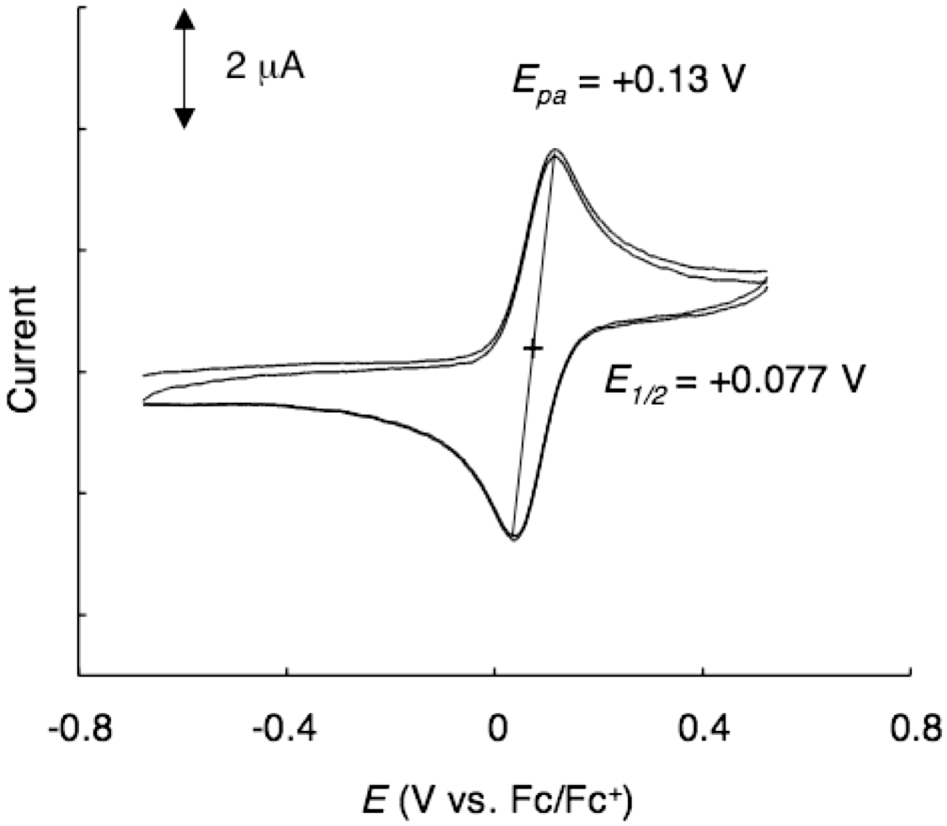

Figure 5

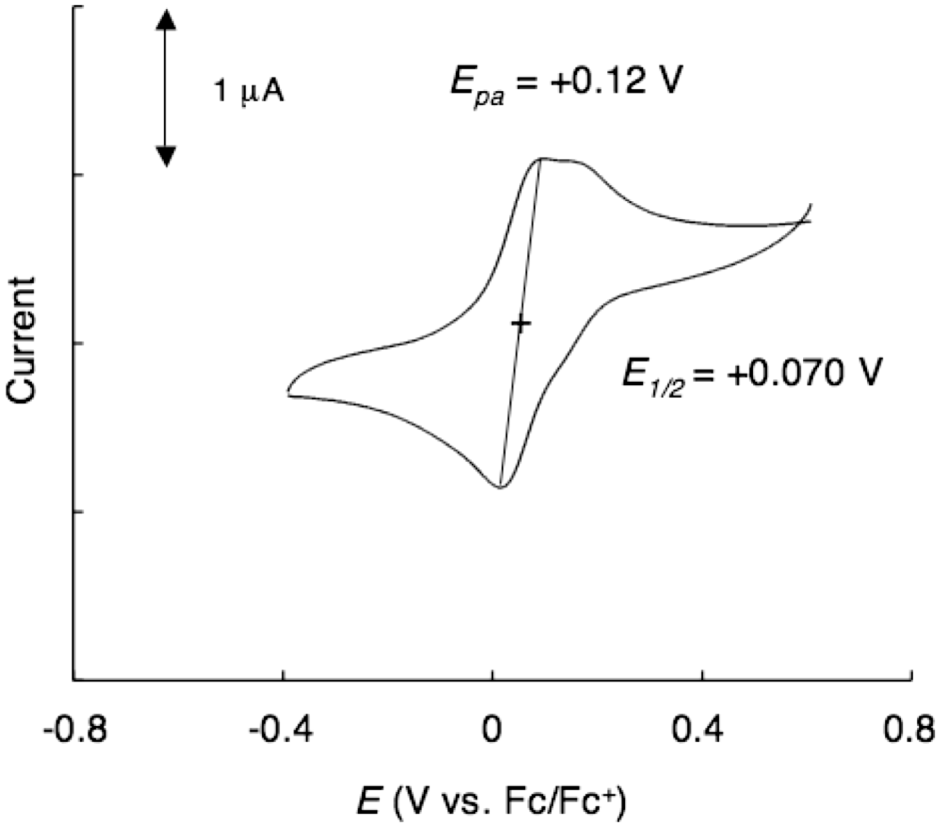

Figure 6

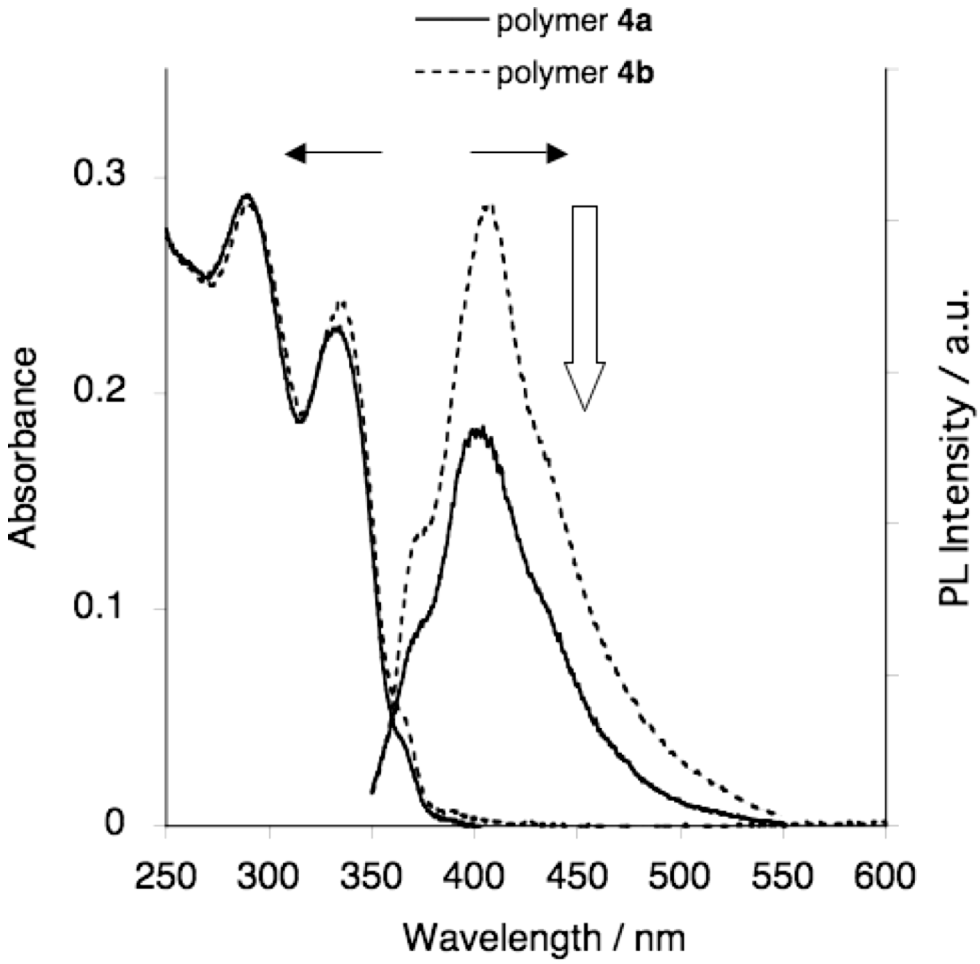

Figure 7

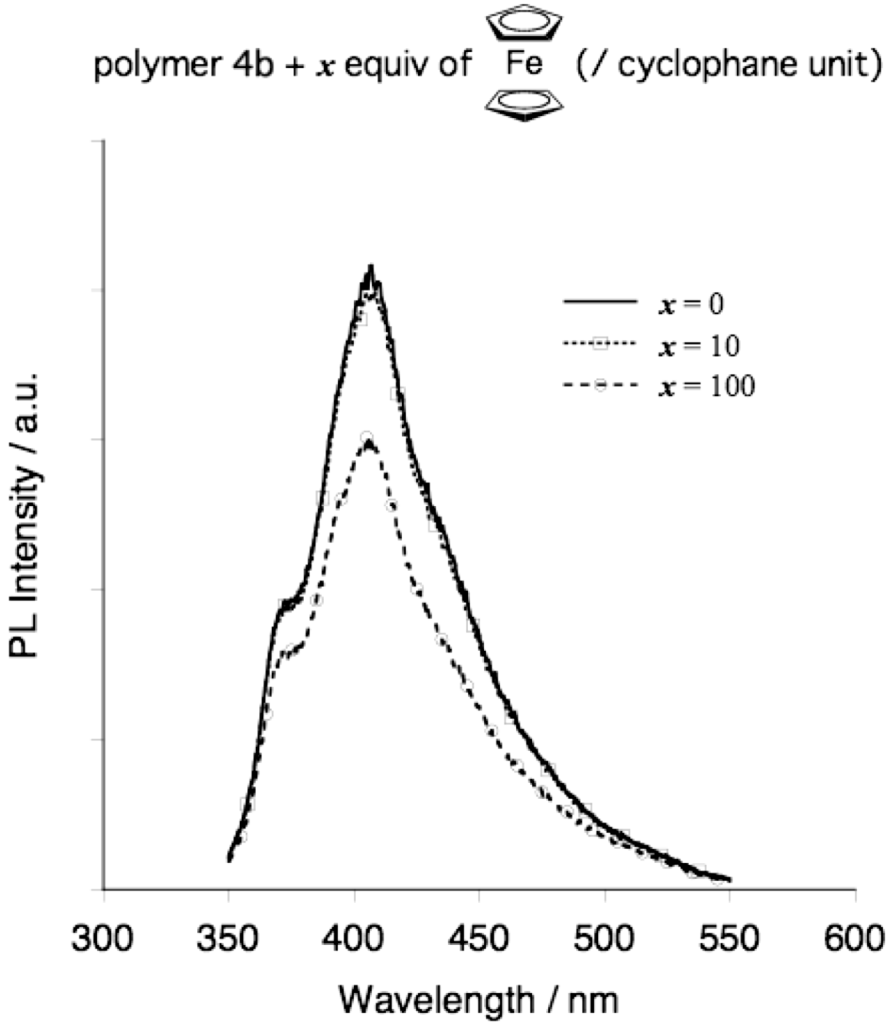

Figure 8